JOURNAL OF
biomaterials applications

Journal of Biomaterials Applications
2015, Vol. 29(6) 791–800

DOI: 10.1177/0885328214548693
jba.sagepub.com
SAGE

Microstructural modifications induced by accelerated aging and lipid absorption in remelted and annealed UHMWPEs for total hip arthroplasty

Leonardo Puppulin[1], Wenliang Zhu[2], Nobuhiko Sugano[2] and Giuseppe Pezzotti[3,4]

Abstract

Three types of commercially available ultra-high molecular weight polyethylene (UHMWPE) acetabular cups currently used in total hip arthroplasty have been studied by means of Raman micro-spectroscopy to unfold the microstructural modification induced by the oxidative degradation after accelerated aging with and without lipid absorption. The three investigated materials were produced by three different manufacturing procedures, as follows: irradiation followed by remelting, one-step irradiation followed by annealing, 3-step irradiation and annealing. Clear microstructural differences were observed in terms of phase contents (i.e. amorphous, crystalline and intermediate phase fraction). The three-step annealed material showed the highest crystallinity fraction in the bulk, while the remelted polyethylene is clearly characterized by the lowest content of crystalline phase and the highest content of amorphous phase. After accelerated aging either with or without lipids, the amount of amorphous phase decreased in all the samples as a consequence of the oxidation-induced recrystallization. The most remarkable variations of phase contents were detected in the remelted and in the single-step annealed materials. The presence of lipids triggered oxidative degradation especially in the remelted polyethylene. Such experimental evidence might be explained by the highest amount of amorphous phase in which lipids can be absorbed prior to accelerated aging. The results of these spectroscopic characterizations help to rationalize the complex effect of different irradiation and post-irradiation treatments on the UHMWPE microstructure and gives useful information on how significantly any single step of the manufacturing procedures might affect the oxidative degradation of the polymer.

Keywords

Polyethylene, lipid absorption, hip replacement, oxidation, Raman spectroscopy

Introduction

Acetabular cups of modern hip implants are manufactured from ultra-high-molecular-weight polyethylene (UHMWPE), a material with extreme durability in its non-oxidized state.[1] However, polymer engineers and scientists have long studied methods to concurrently improve wear resistance, deformation/fracture resistance and oxidative stability of UHMWPE by varying manufacturing methods, consolidation techniques, resin recipes, bearing surface treatment (e.g. laser-assisted ion implantation or coating with cross-linked polyethylene glycol (PEG) to improve wear resistance), or reinforcing the polyethylene matrix with carbon fibers. Studies dating back to the 1990s clearly proved that the use of ionizing radiation to crosslink the polymeric chains effectively could reduce adhesive/abrasive wear of UHMWPE bearings.[2–4] However, more recent studies have shown that the performance

[1]Department of Molecular Cell Physiology, Kyoto Prefectural University of Medicine, Kamigyo-ku Hirokoji Agaru, Kyoto, Japan
[2]Department of Orthopedic Surgery, Osaka University Medical School, 2-2 Yamadaoka, Suita 565-0871 Osaka, Japan
[3]Ceramic Physics Laboratory and Research Institute for Nanoscience, Kyoto Institute of Technology, Sakyo-ku, Kyoto, Japan
[4]The Center for Advanced Medical Engineering and Informatics, Osaka University, Yamadaoka, Osaka, Japan

Corresponding author:
Giuseppe Pezzotti, Ceramic Physics Laboratory and Research Institute for Nanoscience, Kyoto Institute of Technology, Sakyo-ku, Kyoto, Japan.
Email: pezzotti@kit.ac.jp

of conventional gamma-sterilized UHMWPE is excellent during the first decade of implantation of the bearing component, while wear and oxidation might become an issue for the mechanico-chemical stability of the material starting from the beginning of the second decade. In fact, the irradiation causes hemolytic cleavage of C-C and C-H bonds of the polyethylene molecular chains. The resulting alky radicals are not stable and enter a complex system of reactions, which not only lead to crosslinking in the amorphous phase, but also to chain scissions, oxidation, formation of C=C double bonds and transformations to more stable allyl and peroxy radicals. The formation of C=C double bonds is not assumed to have a significant effect on the performance of the polymer, but all the other reactions influence wear and mechanical properties adversely.[5,6] Chain scission leads to lower molecular weight polyethylene, whose wear and mechanical performances are inferior as compared to the original polymer. In the effort of counteract such a degradation of the material, combining irradiation process with a post-irradiation annealing to eliminate residual free radicals has been identified as the solution to improve wear and oxidation resistance.[7–11] In a recent publication, Oral et al. reported an interesting study in which oxidative degradation of irradiated and melted UHMWPE components was observed as a consequence of exposition to body fluids during shelf-aging.[12] The absorption of lipids, which are present in the synovial fluid and are in contact with the polyethylene component during implantation, might trigger accelerated oxidation and degradation of the mechanical properties of these materials. The oxidation rate is dependent on lipid concentration, oxygen concentration, and temperature. Diffusion of lipids in the semicrystalline polymer induces plasticization, especially on the surface where the concentration of absorbed species reaches its highest value. In turn, plasticized polymers show deterioration of wear resistance, whose extent depends on the nature and the amount of the lipids.[13,14] Although Greenbaum et al.[15] did not notice any reduction of wear resistance in their *in vitro* experiments on polyethylene with absorption of lipids, they confirmed the deterioration of some mechanical properties (significant reduction of compressive elastic modulus and compressive yield strength). The debate regarding these important issues, recently brought to the consideration of the scientific community, made clear that a comprehensive characterization of the response to oxidation of the new generation UHMWPEs is still lacking. In other words, the idea of removing the free radicals generated during processing might not be sufficient to guarantee a bearing component immune to long-term oxidation if the microstructure of the material is prone to absorb a conspicuous amount of lipids and if the initial density of residual free radical is high.

The purpose of this study was to investigate the microstructural modifications induced by accelerated aging in three different (commercially available) highly crosslinked UHMWPEs which where *in vitro* oxidized with and without the presence of absorbed lipids in their microstructure. Two materials belonged to an early generation single-step irradiated polyethylene (Crossfire^{TM}, Stryker Orthopaedics, Inc., Mahwah, NJ and Longevity^{TM}, Zimmer, Inc., Warsaw, IN, USA), while the third investigated material belonged to a successive generation of sequentially irradiated polyethylene (X3^{TM}, Stryker Orthopaedics, Inc., Mahwah, NJ, USA).

Materials and methods

UHMWPE materials

Three commercially available liners were investigated in the present study. The main characteristics and peculiarities of the three materials, including the steps of the processing, can be summarized as follow:

(1) Longevity^{TM}, hereafter referred as Liner A, is manufactured by Zimmer, Inc. (Warsaw, IN, USA) and it is a first-generation remelted liner clinically introduced in the Trilogy acetabular cup design since 1999. Molded sheets, consolidated from GUR 1050 resin (5.5–6 million g/mol), are radiation crosslinked by electron beam with a total dose of 100 kGy and then remelted (>135°C) to quench residual free radicals.
(2) Crossfire^{TM}, hereafter referred as Liner B, is manufactured by Stryker Orthopedics, Inc. (Mahwah, NJ, USA). This brand also belongs to the first-generation of annealed liners. This liner was clinically introduced in 1998. The manufacturing procedure of Crossfire^{TM} also starts from GUR 1050 resin but the resin has the morphology of extruded rods. The rods are gamma-irradiated with a nominal dose of 75 kGy and subsequently annealed at 130°C. After being machined into liner shape and then barrier packaged, Crossfire^{TM} is exposed again to gamma irradiation for sterilization purpose with the nominal dose of 30 kGy in nitrogen atmosphere.
(3) X3^{TM}, hereafter referred as Liner C, is manufactured by Stryker Orthopedics, Inc. (Mahwah, NJ, USA). It belongs to a second-generation annealed liner and was clinically introduced in the Trident and Tritanium acetabular cup design in 2005. GUR 1020 (3.5 million g/mol) compression molded sheets are gamma irradiated at the nominal dose of 30 kGy and then annealed at 130°C.

The same procedure is sequentially repeated three times (i.e. the cumulative radiation dose being 90 kGy).

The polyethylene liners as received by the manufactures were cut through their thickness to obtain rectangular prisms from the area of the alleged main wear zone (contact area between hip cup and femoral counter surface). In every prism-shaped specimen, one face preserved to the original surface of the liner, as shown in Figure 1(a). For each sample, this area was investigated using confocal Raman microspectroscopy after *in vitro* oxidation. Three cups for each of the three materials were cut and two specimens were obtained from each cup: one specimen underwent accelerated aging while the second one was immerse in lipid solution (squalene) before accelerated aging. The procedure of *in vitro* oxidation and absorption of lipids are described in the next section.

Accelerated aging with and without lipid absorption

The accelerated aging of the samples was performed according to the standards ASTM F2003-02 (reapproved in 2008)[16] with the intent to investigate the oxidative stability of Liners A, B, and C. Following the standard procedures, the three materials were oxidized under equal conditions prior to characterization of their microstructures by Raman spectroscopy. Unlike infrared spectroscopy, Raman spectroscopy allows non-destructive characterization without further sample manipulation. A set of samples obtained from new cups of the three materials were immersed for 4 h in squalene (95% solution, Wako Pure Chemicals Industries, Ltd., Osaka, Japan) at elevated temperature (100°C in a convection oven) to induce diffusion of lipids in the microstructure before accelerated aging. As a lipid to be diffused through the specimens, we chose squalene because it is a precursor in cholesterol synthesis and it is present in the synovial fluid with

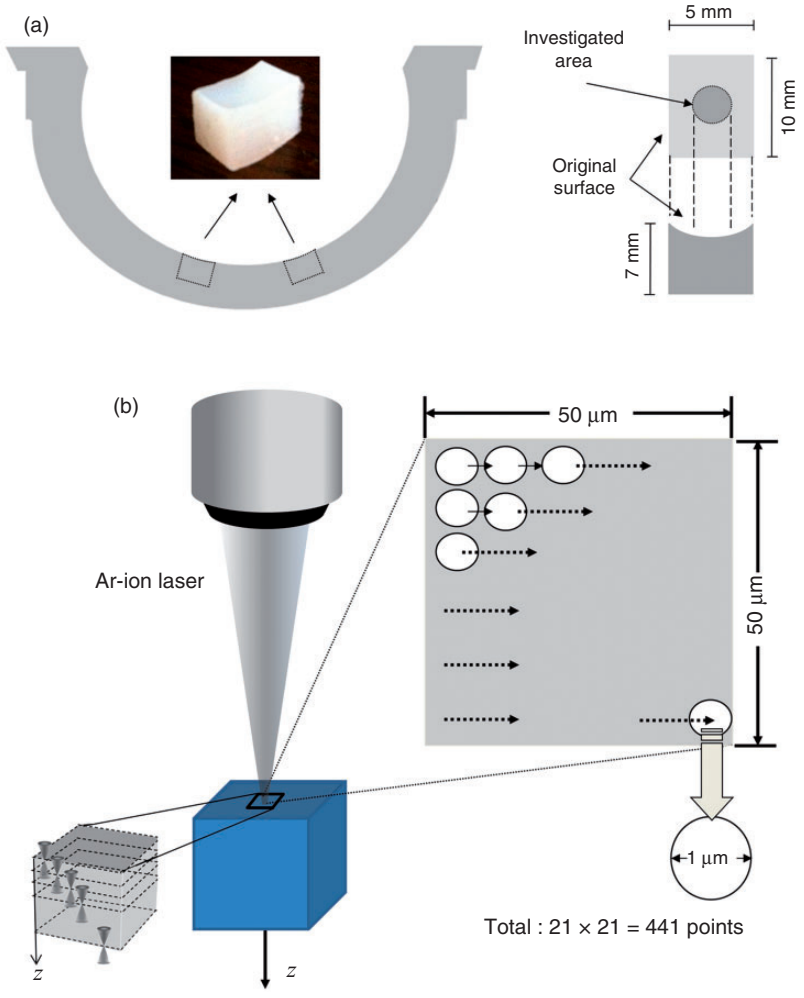

Figure 1. (a) Schematics showing the geometry of the samples for accelerated aging and the locations of the liner from which they were cut. (b) Schematics of the spectroscopic measurement protocol.

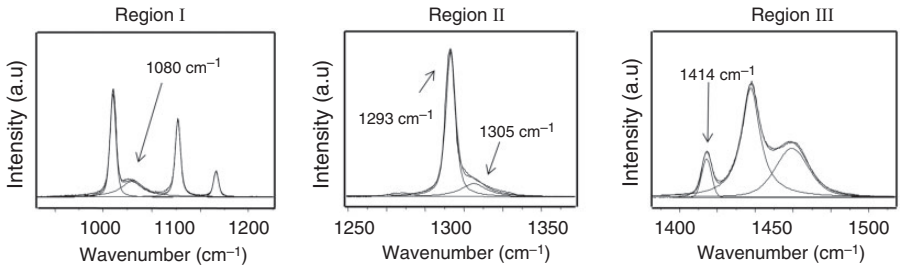

Figure 2. Typical Raman spectrum of polyethylene with its related individual bands after spectral deconvolution. The bands used for the calculation of phase fractions are also labeled.

unsaturated bonds (thus inducing generation of free radicals in UHMWPE during *in vivo* implantation). At the completion of the procedure of lipid diffusion, all specimens were cooled down to room temperature in their respective lipid solution and remnants of the solution were carefully removed from the surface of the samples. Subsequently, all samples (with and without diffused lipids) underwent accelerated aging, whose preliminary conditioning step consisted of irradiating the specimens with γ-ray (25 kGy dose) and maintaining them at 23°C for 28 days. An oxygen bomb was used to age the specimens at 70°C in pure oxygen (5 atm) for 14 days. All the specimens were analyzed by micro-Raman spectroscopy within 10 days after the completion of the test.

Confocal Raman spectroscopy

All the spectroscopic assessments in this study were made by means of a Raman microprobe spectrometer (T-64000, Horiba/Jobin-Yvon, Kyoto, Japan) in back-scattering geometry. The excitation source was a 488.0 nm Ar-ion laser (Stabilite 2017-Spectra Physics, Mountain View, CA) yielding a power of approximately 35 mW on the UHMWPE liner surface. The confocal configuration of the probe adopted throughout the present experiments corresponded to a $100\times$ objective; numerical aperture, focal length, and pinhole diameter were fixed as: NA = 0.9, $f = 11$ mm, and $\Phi = 100\,\mu$m, respectively. Individual spectra were typically collected in 10 s in both polarized and non-polarized measurements. The recorded spectra were averaged over three successive measurements at each selected location. A spectral resolution better than $0.15\,\text{cm}^{-1}$ was achieved by means of an 1800 grating l/mm. Spectral mapping was non-destructively performed in order to characterize crystallinity from the surface down to 100 μm inside of UHMWPE acetabular liners. A map $50\times 50\,\mu\text{m}^2$ in dimension was collected at eight different depths depth ($z_{lab} = 0$, 5, 10, 20, 35, 50, 75 and 100 μm) with an in-plane sampling of 2.5 μm step (for a total of 441 spectra per each map). A schematic of the spectroscopic measurement protocol is given in Figure 1(b). The relationship between the observed Raman bands and the vibrational modes of the polyethylene molecular structure has been amply documented in the literature.[17–23] Figure 2 shows a typical Raman spectrum of polyethylene with its related individual bands after spectral deconvolution. Spectral deconvolution has been performed by means of an automatic fitting algorithm enclosed in a commercially available computational package (Labspec 3, Horiba/Jobin-Yvon, Kyoto, Japan), using mixed Gaussian/Lorentzian curves. The Raman spectrum of polyethylene (shown here in the range between 950 and $1600\,\text{cm}^{-1}$) can be divided into three main regions: *region I*, dominated by the C–C stretching vibrational mode in the interval 1000–$1150\,\text{cm}^{-1}$; *region II*, mainly represented by the $-CH_2-$ twisting vibration at around $1300\,\text{cm}^{-1}$; and *region III*, which is characteristic of $-CH_2-$ bending between 1350 and $1500\,\text{cm}^{-1}$. The broad band at $1080\,\text{cm}^{-1}$ is associated with the presence of an amorphous phase.[21] The peak at $1414\,\text{cm}^{-1}$ is characteristic of an orthorhombic phase, which represents the almost totality of the crystalline phase, and the peak at $1293\,\text{cm}^{-1}$ can be used to approximate the degree of crystallinity of the overall UWMWPE structure.[19–23] The percentages of crystalline (α_c) and amorphous (α_a) phases can be calculated from the Raman spectrum of polyethylene, according to the following equations[21]

$$\alpha_c = \frac{I_{1414}}{0.46(I_{1293} + I_{1305})} \times 100 \quad (1)$$

$$\alpha_a = \frac{I_{1080}}{0.79(I_{1293} + I_{1305})} \times 100 \quad (2)$$

where I is the integral intensity of each individual Raman band identified by the subscript (i.e. after spectral deconvolution). Note also that the sum $(\alpha_a + \alpha_c)$ might locally be <100, because of the possible presence of a minor fraction of matter in an anisotropic intermediate disordered state (i.e. usually referred to as the

Table 1. Specification of the groups (material and treatment), the dependent variables (studied parameters), and the number of measurements used for the statistical analysis.

Material		Treatment	No. of samples	No. measurements per depth	No. measurements per depth-treatment material	No. of depths per sample	Studied parameters
Liner A	Longevity™	Pristine	3	$21 \times 21 = 441$	$441 \times 3 = 1323$	8	α_c, α_a, α_b
		Aging	3	441	1323	8	
		Lipid+aging	3	441	1323	8	
Liner B	Crossfire™	Pristine	3	441	1323	8	
		Aging	3	441	1323	8	
		Lipid+aging	3	441	1323	8	
Liner C	X3™	Pristine	3	441	1323	8	
		Aging	3	441	1323	8	
		Lipid+aging	3	441	1323	8	

α_c: crystalline phase; α_a: amorphous phase; α_b: third phase.

"third phase"[19]). Accordingly, the fraction of this intermediate phase, α_t, can be expressed as follow

$$\alpha_b = 100 - (\alpha_c + \alpha_a) \quad (3)$$

Equations (1) to (3) constitute the basis of the Raman spectroscopic method for characterizing the partially crystalline structures of the UHMWPE.

Statistical analysis

This Raman investigation was designed to find differences among three types of UHMWPE tested in three different oxidative conditions: as received by the manufacturers (controls), as oxidized after accelerated aging, and as oxidized after lipid absorption and accelerated aging. The dependent variables (crystallinity, amorphous and third-phase fractions) were analyzed for statistical significance by analysis of variance (ANOVA). The total number of groups (dependent variables) was set to 9: three types of polyethylene in three different oxidative conditions. For each group, three samples were tested collecting square maps of 21×21 Raman measurements ($n = 441$) at eight different depths. In Table 1 are summarized the groups and the studied parameters as considered in our statistical analysis. Within the same group and at the same depth, one-way ANOVA test results showed that the population means of the three maps were not significantly different ($p > 0.05$ in all cases). Based on this preliminary analysis of the data, we decided to carry on the further statistical tests considering the means and standard deviation as calculated from the three maps for each group and depth. The statistical comparison of the retrieved data was designed as follows: (i) for each group, the variations of calculated phase fraction depending on the depth were verified by one-way ANOVA and post hoc Tukey tests; (ii) comparisons among different materials in different oxidative condition, namely different groups, were performed using one-way ANOVA and post hoc Tukey tests. The data manipulation for statistical analysis was performed using the software Origin Pro 8.5 (OriginLab, NorthAmpton, MA, USA).

Results and discussion

Two-dimensional Raman maps collected at different focal depths, as explained in the Confocal Raman spectroscopy section, enabled to visualize microstructural patterns along the material subsurface. In order to give a statistically meaningful picture of the microstructural conformation of the three materials, we decided to analyze three different samples for each material and specific condition of *in vitro* oxidation. The average values of crystalline, amorphous and third phase as calculated from the three maps were considered in the discussion as the parameters characterizing each liner at each oxidative condition. Although the practice of accelerated aging might not simulate the real degradation occurring in hip components during implantation (e.g. the influence of cycling loading on the resistance to oxidation is not considered), as clearly stated in the ASTM standards themselves, these experimental procedures are extremely substantial and meaningful to judge and discuss the structural modifications induced by the oxidation of different UHMWPE materials as a function of starting resin, consolidation process, sterilization method and post-irradiation treatment. Figure 3 shows in-depth profiles of crystallinity fraction, α_c, as calculated from the three liners at different aging conditions. Specifically, Figure 3(a) to (c) shows

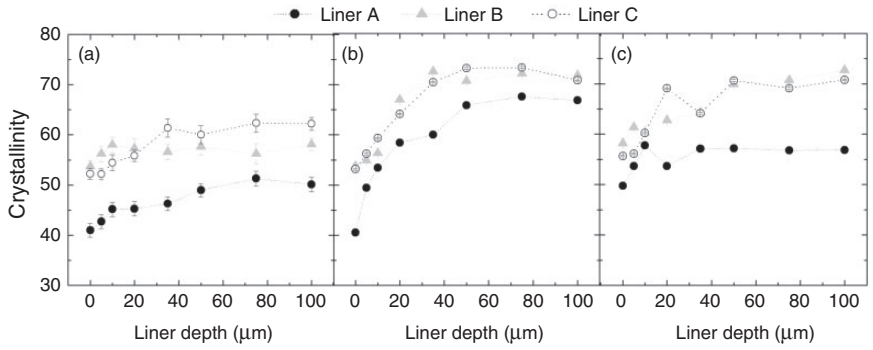

Figure 3. In-depth profiles of crystallinity fractions (% volume) as collected in the three materials at different oxidative conditions: (a) non-oxidized material (Case 1), (b) after accelerated aging (Case 2), and (c) after absorption of lipids and accelerated aging (Case 3).

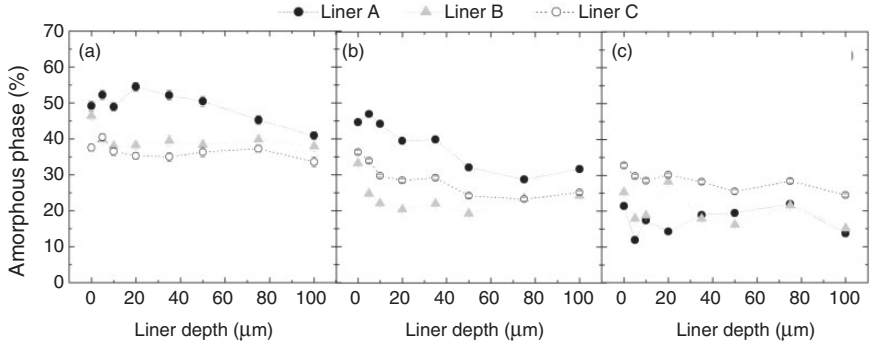

Figure 4. In-depth profiles of amorphous phase fractions (% volume) as collected in the three materials at different oxidative conditions: (a) non-oxidized material (Case 1), (b) after accelerated aging (Case 2), and (c) after absorption of lipids and accelerated aging (Case 3).

the trends of crystalline phase for the three materials in their non-oxidized state (hereafter referred as Case 1), after accelerated aging (hereafter referred as Case 2) and after lipid absorption followed by accelerated aging (hereafter referred as Case 3), respectively. Similarly, Figures 4(a) to (c) and 5(a) to (c) report the trends of amorphous phase fraction, α_a, and third phase fraction, α_t, respectively. The scattering bars represent the standard variations of the calculated means, which were low and reliable in all the cases because of the large number of measurements for each map. For each profile, one-way ANOVA test was performed to confirm the differences among the average values of phase fraction calculated at different depths. In all the profiles showed in Figures (3) to (5), the results of the test confirmed that the population means are different ($p < 0.05$). As far as the crystallinity is concerned, all the three materials revealed gradients of crystallinity along the first microns of the subsurface in all the three cases, with the average lowest values on the surface. The crystalline phase fraction linearly increases along the first microns of the subsurface and it reaches a plateau at around 35–50 μm, but in Cases 2 and 3, such a gradient became steeper. This evidence might prove that in the sub-surface, there is the most favorable trade-off between high concentration of free radicals and oxygen. In Case 1 (Figure 3(a)), the differences among the retrieved profiles can be interpreted as the direct consequence of the selected processing (namely, reduced crystallinity by remelting (Liner A) vs. substantial preservation of the as-irradiated structure upon annealing (Liner B and Liner C)). Moreover, the higher crystallinity in Liner C (62.3%) as compared to Liner B (58.1%) can mainly be explained by considering the lower molecular weight of the resin used in X3^{TM} material (GUR1020 vs. GUR1050). In Cases 2 and 3 (Figure 3(b) and (c)), all the three materials after accelerated aging clearly showed increases of crystallinity underneath the surface (especially deeper than 20 μm), as compared to their respective non-oxidized states (Case 1). On the surface of Liners B and C, the increase of crystallinity is not substantial as in Liner A. In fact, if on one hand, in Liner B the modification induced by oxidation on the surface leads to a robust

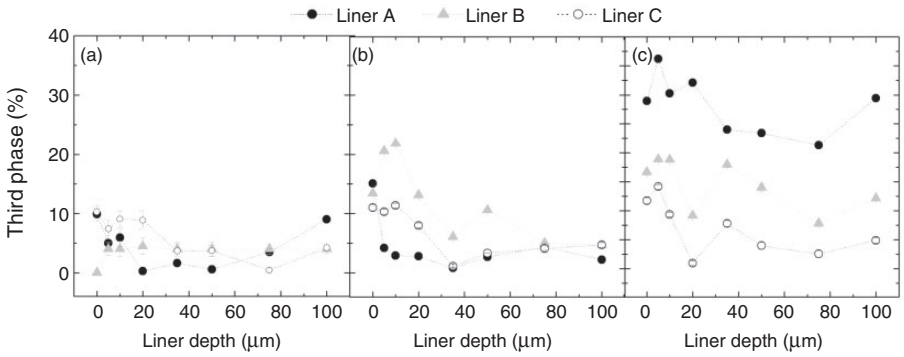

Figure 5. In depth profiles of third phase fractions (% volume) as collected in the three materials at different oxidative conditions: (a) non-oxidized material (Case 1), (b) after accelerated aging (Case 2), and (c) after absorption of lipids and accelerated aging (Case 3).

increase of third phase rather than crystalline phase (see Figure 5), on the other hand, on the surface of Liner C the lowest content of oxygen-rich amorphous phase in the pristine (see Figure 4(a)) and, presumably, the lowest concentration of free radicals might have preserved the microstructure from oxidation. One of the most detrimental effects of oxidation in UHMWPE is the reduction of molecular weight induced by chain scission (triggered by the formation of oxidized products, such as ketones and carboxyl acids). In our *in vitro* degradation experiments, recrystallization is univocally correlated to the shortening of molecular chains, which acquire higher mobility to reorganize in crystalline domains at lower and more stable energy.[23] Moreover, this microstructural modification is promoted and accelerated by the temperature (70°C in our case) and, possibly, by the presence of chemical species such as lipids, which might form new free radicals. In other words, no further external variables had been added to the system under investigation and any observed increase of crystallinity (and third phase content) at the expensive of the amorphous phase should be correlated to the oxidative degradation. It has already been demonstrated in several studies that oxidation leads to deterioration of the mechanical properties, such as loss of ductility (embrittlement) and lower wear resistance.[24–30] Therefore, the variations of phase fractions as calculated by Raman spectroscopy and presented in this paper are directly correlated to the worsening of wear and mechanical properties in UHMWPE. Keeping in mind these considerations, comparison between Case 2 and 3 showed that the presence of lipids promoted recrystallization, namely higher oxidation, after aging in all the investigated materials at their very surface ($z = 0$). Conversely, Case 3 for Liner B and C did not show any remarkable difference in the sub-surface as compared to Case 2, while in Liner A the diffusion of lipids inhibited the formation of crystallinity. In order to understand and discuss the latter experimental evidence, we must take into consideration also the variation of the other two phases in the material. In fact, Figures 4(b) and (c) and 5(b) and (c) show that in Liner A the incorporation of lipids induced an abrupt decrease of amorphous phase followed by and increase of third phase. This phase is considered to be an intermediate phase forming an interfacial layer between crystalline and amorphous material. The molecular chains contained in this layer are stretched, conferring an anisotropic character to this phase and properties that are intermediate between the orthorhombic crystallites and the amorphous material. Strobl and Hagedorn described the third phase as consisting of crystalline-like structures which have lost their lateral order but which cannot simply be identified as another crystal modification.[19] As a matter of fact, lipids diffuse through the amorphous phase,[5] where they can promote the formation of oxidized species. In liner A, the amount of amorphous phase in the pristine is higher than the other two materials (cf. Figure 4(a)), which means that it might have absorbed the highest concentration of lipids. On the other hand, Liner B and C might have incorporated fewer lipids, which could explain the moderate decrease of amorphous phase (especially in Liner C) as compared to Liner A. In addition, oxidation-induced recrystallization in the amorphous phase of Liner A might have been impeded by the higher concentration of lipids, which, in turn, led to the formation of new third phase rather than a perfectly ordered orthorhombic crystallographic structure. In Figure 6(a) to (c), Cases 2 and 3 are compared in terms of variation from the non-oxidized state (Case 1) of crystallinity, amorphous phase, and third phase, respectively, as retrieved from the bulk of the three materials. We considered as representative of the bulk the average calculated from the maps collected at 50, 75, and 100 μm in depth. One-way ANOVA tests and post hoc Tukey tests confirmed

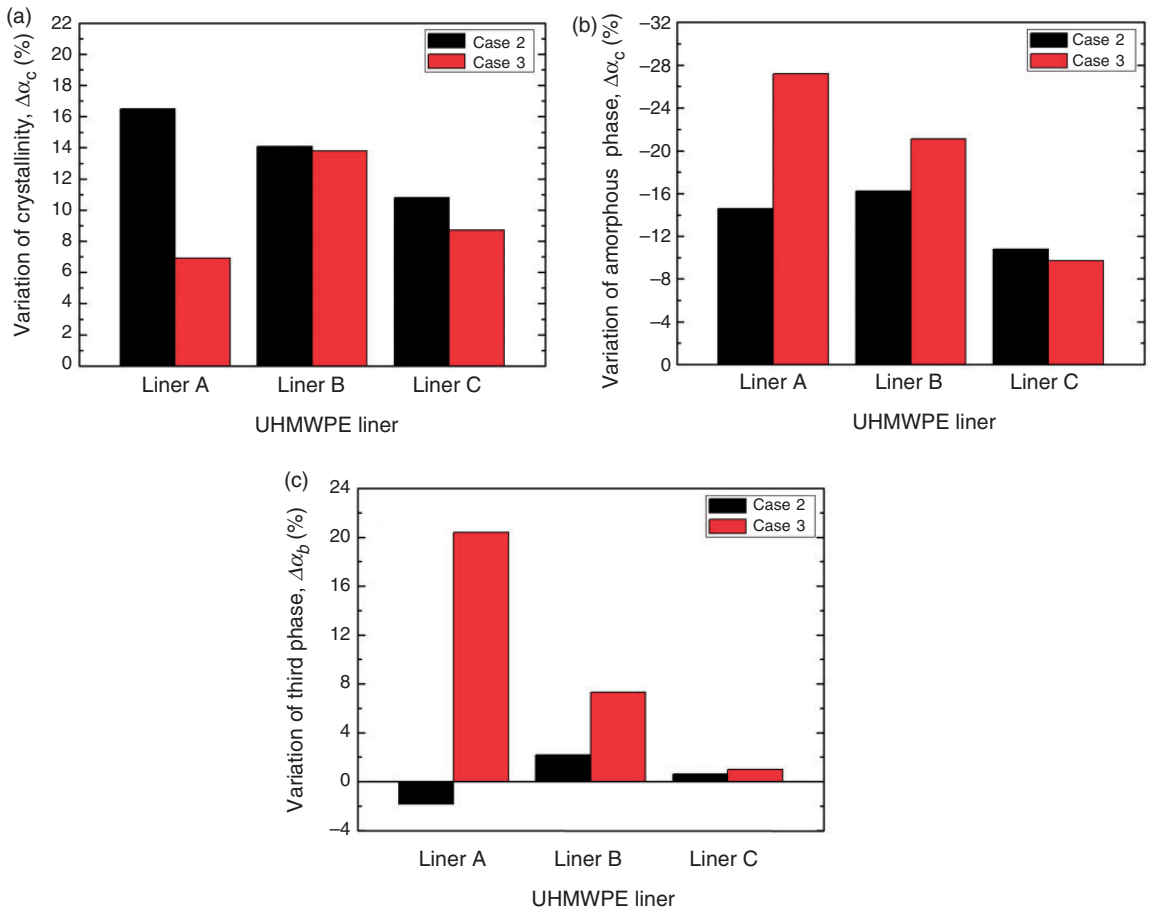

Figure 6. (a) Variation of bulk crystallinity for the three liners under investigation after accelerated aging (Case 2) and after aging with lipid absorption (Case 3). (b) Variation of bulk amorphous phase for the three liners under investigation after accelerated aging (Case 2) and after aging with lipid absorption (Case3). (c) Variation of bulk third phase for the three liners under investigation after accelerated aging (Case 2) and after aging with lipid absorption (Case 3).

that the population means plotted in Figures 3–5 are statistically different ($p < 0.05$).

In Case 2, namely the samples that underwent accelerated oxidation without lipids, Liner A experienced the highest variation of crystallinity, while Liner C the lowest one. Concurrently, Liner C showed lowest variation of amorphous and third phases. Liner B showed a similar trend to Liner A in Case 2, although an interesting difference is worthy to remark: in both materials the reduction of amorphous phase is similar, but in Line A also part of the third phase transformed to crystalline phase (cf. Figure 6(c), showing third-phase decrease in Liner A). We might hypothesize that free radicals were trapped also in the intermediate phase of the initial microstructure of Liner A leading to oxidation and subsequent transformation to crystalline phase. In Case 3, as previously discussed comparing the in-depth profiles, the most striking evidence resided in the lowest variation of crystallinity of Liner A (cf. Figure 6(a)), but, conversely, the most remarkable reduction of amorphous phase and increase of third phase as compared to Liners B and C (cf. Figure 6(b) and (c)). In presence of lipids, Liner B showed a higher reduction of amorphous phase and, similarly to Liner A, formation of third phase was promoted. Liner C showed the lowest variation of the three phases also in Case 3 runs. Comparing Cases 2 and 3 for Liner C, it is clear that the presence of lipids did not affect the oxidative resistance of the polymer, presumably due to the combined effect of low starting concentration of free radicals and the small fraction of amorphous phase in which lipids can be absorbed.

Conclusions

In accelerated oxidation without lipids, the three-step annealed highly crosslinked UHMWPE experienced the lowest variation of crystalline, amorphous and third phases. The two materials belonging to the first generation of highly crosslinked UHMWPE showed similar trends for phase-fraction variation induced by *in vitro* oxidative degradation: the total decrease of amorphous

phase in which oxidized species are formed is slightly superior for the single-step annealed material as compared to the remelted one, presumably due to the lower concentrations of free radicals in the remelted material. Also in lipid-assisted accelerated oxidation, the new generation of highly crosslinked polyethylene showed the lowest (total) variation of the three phases: the presence of lipids did not affect the oxidative resistance of the polymer, presumably due to the combined effect of its low starting concentration of free radicals and the low amorphous phase in which lipids could be absorbed. The latter hypothesis seems to be confirmed by the observation that, in the remelted material, the oxidative stability given by the initial low concentration of free radicals seems to be offset by the highest amount of amorphous phase in which lipid absorption is favored. The microstructure of the new generation 3-step annealed material was thus found to be the most stable as compared to previous generation remelted and single-step annealed polyethylenes.

Declaration of conflicting interests

None declared.

Funding

This research received no specific grant from any funding agency in the public, commercial, or not-for-profit sectors.

References

1. Sutula LC, Collier JP, Saum KA, et al. Impact of sterilization on clinical performance of polyethylene in the hip. *Clin Orthop* 1995; 319: 28.
2. Oonishi H, Kuno M, Tsuji E, et al. The optimum dose of gamma radiation-heavy doses to low wear to low wear polyethylene in total hip prostheses. *J Mater Sci: Mater Med* 1997; 8: 11–18.
3. Bargmann LS, Bargmann BC, Collier JP, et al. Current sterilization and packaging methods for polyethylene. *Clin Orthop* 1999; 369: 49–58.
4. McKellop H, Shen F, Lu B, et al. Development of an extremely wear-resistant ultra high molecular weight polyethylene for total hip replacement. *J Orthop Res* 1999; 17: 157–167.
5. Costa L, Carpentieri I and Bracco P. Post electron-beam irradiation oxidation of orthopaedic UHMWPE. *Polym Degrad Stabil* 2008; 93: 1695–1703.
6. Costa L and Bracco P. Mechanisms of crosslinking, oxidative degradation and stabilization of UHMWPE. In: Kurtz SM (ed.) *UHMWPE Biomaterilas handbook*, 2nd ed., Chapter 21, London: Elsevier, 2009, pp.329–323.
7. Kurtz SM, Orhum OK, Evans M, et al. Advances in the processing, sterilization, and crosslinking of ultra-high molecular weight polyethylene for total joint arthroplasty. *Biomaterials* 1999; 20: 1659–1688.
8. Kurtz SM, Mazzucco D, Rimnac CM, et al. Anisotropy and oxidative resistance of highly crosslinked UHMWPE after deformation processing by solid-state ram extrusion. *Biomaterials* 2006; 27: 24–34.
9. Dumbleton JH, D'Antonio JA, Manley MT, et al. The basis for a second-generation highly crosslinked UHMWPE. *Clin Orthop Relat Res* 2006; 453: 265–271.
10. Wang A, Zeng H, Yau SS, et al. Oxidation and mechanical properties of a sequentially irradiated and annealed UHMWPE in total joint replacement. *J Phys D Appl Phys* 2006; 39: 3213–3219.
11. Morrison ML and Jani S. Evaluation of sequentially crosslinked ultra-high molecular weight polyethylene. *J Biomed Mater Res B Appl Biomater* 2009; 90: 87–100.
12. Oral E, Ghali BW, Neils A, et al. A new mechanism of oxidation in ultrahigh molecular weight polyethylene caused by squalene absorption. *J Biomed Mater Res B Appl Biomater* 2012; 100: 742–751.
13. Costa L, Bracco P, Brach del Prever E, et al. Analysis of products diffused into UHMWPE prosthetic components in vivo. *Biomaterials* 2001; 22: 307–315.
14. Lancaster JK. *Encyclopaedia of polymer science and engineering,* Vol 1. New York: Wiley, 1985, p.12.
15. Greenbaum ES, Burroughs BB, Harris WH, et al. Effect of lipid absorption on wear and compressive properties of unirradiated and highly crosslinked UHMWPE: an in vitro experimental model. *Biomaterials* 2004; 25: 4479–4484.
16. ASTM Standard F2183-02, 2008. *Standard test method for small punch testing of ultra-high molecular weight polyethylene used in surgical implants*. West Consho-hocken, (PA: ASTM International, 2008.
17. Taddei P, Affatato S, Fagnano C, et al. Vibrational spectroscopy of ultra-high molecular weight polyethylene hip prostheses: influence of the sterilization method on crystallinity and surface oxidation. *J Mol Struct* 2002; 613: 121–129.
18. Mutter R, Stille W and Strobl GR. Transition regions and surface melting in partially crystalline polyethylene: a Raman spectroscopic study. *J Polym Sci B Polym Phys* 1993; 31: 99–105.
19. Strobl GR and Hagedorn W. Raman spectroscopic method for determining the crystallinity of polyethylene. *J Polym Sci: Polym Phys Ed* 1978; 16: 1181–1193.
20. Rull F, Prieto AC, Casado JM, et al. Estimation of crystallinity in polyethylene by Raman spectroscopy. *J Raman Spectr* 1993; 24: 545–550.
21. Glotin M and Mandelkern L. A Raman spectroscopic study of the morphological structure of the polyethylenes. *Colloid Polym Sci* 1982; 260: 182.
22. Nylor CC, Meier RJ, Kip BJ, et al. Raman spectroscopy employed for the determination of the intermediate phase in polyethylene. *Macromolecules* 1995; 28: 2969–2978.
23. Wannomae KK, Bhattacharyya S, Freiberg A, et al. In vivo oxidation of retrieved cross-linked ultra–high-molecular-weight polyethylene acetabular components with residual free radicals. *J Arthroplasty* 2006; 21(7): 1005–1011.
24. Kurtz SM, Hozack W, Marcolongo M, et al. Degradation of mechanical properties of UHMWPE

acetabular liners following long-term implantation. *J Arthroplasty* 2003; 18: 68–78.
25. Collier JP, Sperling DK, Currier JH, et al. Impact of gamma sterilization on clinical performance of polyethylene in the knee. *J Arthroplasty* 1996; 11: 377–389.
26. Currier BH, Currier JH, Collier JP, et al. Shelf life and in vivo duration. Impacts on performance of tibial bearings. *Clin Orthop* 1997; 342: 111–122.
27. Currier BH, Currier JH, Collier JP, et al. Effect of fabrication method and resin type on performance of tibial bearings. *J Biomed Mater Res* 2000; 53: 143–151.
28. Besong AA, Hailey JL, Ingham E, et al. A study of the combined effects of shelf ageing following irradiation in air and counterface roughness on the wear of UHMWPE. *Biomed Mater Eng* 1997; 7: 59–65.
29. Kurtz SM, Bartel DL and Rimnac CM. Post-irradiation aging affects the stresses and strains in UHMWPE components for total joint replacement. *Clin Orthop* 1998; 350: 209–220.
30. Edidin AA, Jewett CW, Kwarteng K, et al. Degradation of mechanical behavior in UHMWPE after natural and accelerated aging. *Biomaterials* 2000; 21: 1451–1460.